Journal of Superconductivity and Novel Magnetism

Field-dependent behavior of AC Susceptibility in [Y0.8Ca0.2](Ba0.5Sr0.5)2Cu3O7-δ

--Manuscript Draft--

Manuscript Number:	JOSC-D-15-00400
Full Title:	Field-dependent behavior of AC Susceptibility in [Y0.8Ca0.2](Ba0.5Sr0.5)2Cu3O7-δ
Article Type:	Original Research
Keywords:	Rietveld refinement, [Y0.8Ca0.2](Ba0.5Sr0.5)2Cu3O7-δ, AC susceptibility
Corresponding Author:	DOW Lee, Ph.D Samsung Advanced Institute of Technology Suwon, KOREA, REPUBLIC OF
Corresponding Author Secondary Information:	
Corresponding Author's Institution:	Samsung Advanced Institute of Technology
Corresponding Author's Secondary Institution:	
First Author:	DOW Lee, Ph.D
First Author Secondary Information:	
Order of Authors:	DOW Lee, Ph.D
	Jiwon Seo
	Luis de los Santos Valladares
	Angel Bustamante Domínguez
	A.M. Osorio Anaya
	Crispin Barns
Order of Authors Secondary Information:	
Funding Information:	National Research Foundation of President Post-doctoral fellowship Program (NRF-2013R1A6A3A060443) — Jiwon Seo
	Superior Council of Research of the National University of San Marcos (151301031) — Angel Bustamante Domínguez

Noname manuscript No.
(will be inserted by the editor)

Field-dependent behavior of AC Susceptibility in $[Y_{0.8}Ca_{0.2}](Ba_{0.5}Sr_{0.5})_2Cu_3O_{7-\delta}$

Dongwook Lee* · Jiwon Seo* · Luis de los Santos Valladares · Angel Bustamante Domínguez · A. M. Osorio Anaya · and Crispin H. W. Barns

Received: date / Accepted: date

Abstract The AC susceptibility of $[Y_{0.8}Ca_{0.2}](Ba_{0.5}Sr_{0.5})_2Cu_3O_{7-\delta}$ was investigated as a function of frequency and amplitude of AC magnetic field. The susceptibilities of the sample display the field amplitude dependence. The peak temperature (T_p) of its imaginary part shows not frequency dependence but field amplitude dependence. The frequency effect on AC susceptibility was negligible. As the field amplitude increases, T_p shifts to lower temperature.

Dongwook Lee
Department of Physics, University of Cambridge, J.J. Thomson Avenue, Cambridge CB3 0HE, United Kingdom
Physics and Applied Physics, School of Physical & Mathematical Sciences, Nanyang Technological University, 637371 Singapore
E-mail: dongwookleedl324@gmail.com

Jiwon Seo
Department of Physics, University of Cambridge, J.J. Thomson Avenue, Cambridge CB3 0HE, United Kingdom
Department of Physics and IPAP, Yonsei University, Seoul 120-749, Republic of Korea
E-mail: jiwonseo@yonsei.ac.kr

Luis de los Santos Valladares
Department of Physics, University of Cambridge, J.J. Thomson Avenue, Cambridge CB3 0HE, United Kingdom

Angel Bustamante Domínguez
Laboratorio de Cerámicos y Nanomateriales, Facultad de Ciencias Físicas, Universidad Nacional Mayor de San Marcos, Ap. Postal 14-0149, Lima, Perú

A. M. Osorio Anaya
Laboratorio de Sol Gel, Facultad de Química e Ingeniería Química, Universidad Nacional Mayor de San Marcos, Av. Venezuela s/n, cdra 34, Ciudad Universitaria, Lima, Perú

Crispin H. W. Barns
Department of Physics, University of Cambridge, J. J. Thomson Avenue, Cambridge CB3 0HE, United Kingdom

This effect can be interpreted in terms of bulk pinning hysteresis loss due to the vortices motion in/out grain boundary.

Keywords $[Y_{0.8}Ca_{0.2}](Ba_{0.5}Sr_{0.5})_2Cu_3O_{7-\delta}$ · AC susceptibility · Rietveld refinement

1 Introduction

Since the discovery of $YBa_2Cu_3O_{7-\delta}$ (YBCO) [1], research on enhancing the critical temperature (T_C) of YBCO has been extensively carried out by rare-earth elements and/or transition metal atoms substitutions [2,3]. Substitution of Y^{3+} by Ca^{2+} increases carrier concentration and has an influence on the charge transfer from Cu-O chains to the CuO_2 layers, which suppress the T_C from 90K to 80K depending on the concentration of Ca atoms [2,3], while the substitution of Sr^{3+} on the Ba site influences mobile hole concentration by charge-transfer from CuO_2 plane, which also changes T_C [4,5]. In addition, study on superconducting properties and ac loss of YBCO and one-site doped YBCO has been enormously performed with AC susceptibility measurements [6,8]. AC susceptibility ($\chi = \chi^{'} + i\chi^{"}$) measurements with high T_C superconductors have been widely used as a powerful tool to investigate superconducting properties such as magnetization, critical currents, order parameter, conductivity, and so on [9,10]. The real part ($\chi^{'}$) represents transition from near-perfect screening to complete penetration of external AC magnetic field into the sample. The peak of the imaginary part ($\chi^{"}$) represents the bulk pinning hysteresis losses in the sample due to the vortices motion in/out grain boundary [11,12]. Pinning losses are less dependent on the frequency of the field but rely on the field amplitude, while the flux losses depend on the frequency, not on the field amplitude [13]. YBCO has frequency dependence, i.e. flux flow motion plays an important role in its AC loss [7,14–16]. In addition, Ca-doped YBCO has similar behavior [17]. However, study on the A-site and B-site co-doped YBCO has not been made so much because 2-site doping YBCO is too difficult. We prepared $[Y_{0.8}Ca_{0.2}](Ba_{0.5}Sr_{0.5})_2Cu_3O_{7-\delta}$ by sol-gel method. Thus, the research on AC susceptibilities of $[Y_{0.8}Ca_{0.2}](Ba_{0.5}Sr_{0.5})_2Cu_3O_{7-\delta}$ [18-20] would reveal the AC loss mechanism of high Tc superconductors. Here, we report that $[Y_{0.8}Ca_{0.2}](Ba_{0.5}Sr_{0.5})_2Cu_3O_{7-\delta}$ shows not frequency dependence but field dependence behavior. The bulk pinning losses in the sample due to the vortices motion in/out grain boundary cause field dependence.

2 Material and methods

The sample was prepared by the Sol-Gel method. In brief, acetates of yttrium, calcium, barium, strontium and copper were mixed stoichiometrically in oxalic acid HCOO-COOH. By metathesis reaction between the solution of the acetates and the oxalic acid in magnetic stirring, we achieved the formation of Y, Ca, Ba, Sr and Cu oxalates. These precursor were calcined at

860°C and sintered at 880°C in a tubular oven LENTON LTF & PTF model 16/610 in oxygen flow to form a powder of $[Y_{0.8}Ca_{0.2}](Ba_{0.5}Sr_{0.5})_2Cu_3O_{7-\delta}$. The sample was characterized by X-ray diffraction using a powder universal diffractometer, Rigaku HGZ in Bragg-Brentano geometry. We use the Cu-Kα1 and Cu-Kα2 radiations with wavelength 1.5405Åand 1.5443Å(ratio 1:1) and step of 0.02°. The Rietveld refinements of the XRD were processed by using the software FullProf v. 2012 [21-22]. The morphological properties of the sample were also characterized by Transmission electron microscope (FEI Philips Tecnai 20). The magnetic properties of the superconductor were studied by Quantum Design MPMS-XL system with option M120 for AC susceptibility measurement.

3 Results and discussions

Figure 1 shows XRD of the sample. The Rietveld refinement was performed by taking the structure of the YBCO (Pmmm) as a model. The red line in the figure represents the best calculated fitting (χ^2= 1.69). The crystal structure is modelled in the inset figure and the cell parameters and atomic positions are listed in Table 1. Note that the cell parameters of the undoped YBCO are: a=3.8206Å, b=3.8851Åand c= 11.6757Å[23,24], giving a volume of 173.30$Å^3$, and orthorhombicity (2(b-a)/(a+b)100%) of 1.67% and cubicity (2(c-a)/(a+c)100%) of 101.38%. The smaller volume for the doped YBCO found here (170.47$Å^3$) is caused by the differences between the ionic radios. In the structure, Y^{3+} and Ba^{2+} share the same position to Ca^{2+} and Sr^{3+} respectively and they are sandwiched by the CuO_2 planes. Despite that the ionic radius of Ca^{2+} (0.99Å) is bigger than the Y^{3+} (0.93Å)) which causes the separation between the superconducting planes, especially between the atoms O2 and O3, the opposite occurs for the case of Sr^{3+} whose ionic radio (1.13Å) is smaller than the one of Ba^{2+} (1.35Å). In this way the b and c dimensions of the perovskites containing the latest atoms become smaller leading in the decrease of the orthorhombicity 0.35% and cubicity 100.18% for our doped YBCO. Figure 2 illustrates the morphological properties of $[Y_{0.8}Ca_{0.2}](Ba_{0.5}Sr_{0.5})_2Cu_3O_{7-\delta}$. The layer structure of the sample is clearly visible in Fig. 2. Stripe patterns reveal that $[Y_{0.8}Ca_{0.2}](Ba_{0.5}Sr_{0.5})_2Cu_3O_{7-\delta}$ layers are parallel and it is crystalline. ED patterns show distinct spots and also halo-like circle, implying that the sample has crystalline phase and there is some less-crystalline region in the sample. Figure 3 displays the susceptibility vs temperature curves of the sample in zero-field cooled mode (ZFC) and field cooled mode (FC). The sample was first cooled down to 7 K in a zero field. After the temperature became stable at 7 K, 25 Oe of DC magnetic field was applied to the sample. With the increase of temperature, the susceptibility of the sample was measured (ZFC). At 150 K, the sample was cooled down again with the applied field. The susceptibility of the sample was recorded again (FC). The sample shows field-irreversibility below 77K, which is Tc, as shown in Fig. 3. Figure 4 shows both real and imaginary parts of AC

susceptibilities at different magnetic field amplitudes as the AC frequencies vary. Although the applied AC field frequencies vary, the real and imaginary parts of the susceptibilities curves seem to be independent of the frequencies. Each imaginary curve shows maximum peak position (T_p). However, T_p does not move with regard to the AC field frequency. Figure 5 shows the real parts of AC susceptibilities at different frequencies with varying AC magnetic field amplitudes. At each fixed frequency, the real part of the susceptibilities curves move upward as the applied AC field amplitudes increase, i.e. the magnitude of the susceptibilities decreases with the increase of the AC field amplitude. Figure 6 illustrates the imaginary part of the AC susceptibilities of the sample at different frequencies with varying AC magnetic field amplitudes. Each curve shows T_p. T_p moves toward lower temperature as the AC field amplitudes increase. In addition, the peak of $\chi^{"}$ also broadens with the decrease of T_p. This is because larger screening currents are required to shield the applied field. Therefore, the T_p of $\chi^{"}$ shifts to lower temperature according to the critical-state model [25]. Moreover, the peak height of $\chi^{"}$ increases as the field amplitude increases like YBCO [26]. According to the critical-state model, the peak of $\chi^{"}$ versus temperature is defined as the temperature at which AC magnetic field flux penetrates to the center of the superconductor. The peaks represent the losses of the shielding current flows within the individual grains. As the driving field amplitude increases larger, larger screening curves are required to shield the applied field. Figure 7 illustrates the variation of T_p with varying AC field amplitudes and frequencies. The magnitude of T_p exponentially decreases as the AC field amplitude increases, as shown in Fig. 7(a). The curves were fitted with an exponential function, as following form. T_p = A + $T_{P0} * exp(-(H_{ac} - H)/H_{ac}))$, where A is a constant, TP0 is a value of T_p with 0 Oe, H_{ac} is the actually-applied field amplitude and H is the field amplitude. Although the sample show field amplitude dependence, it does not show clear dependence on frequency while YBCO single crystal show frequency dependence behavior [27]. To check out whether the sample show frequency dependence or not, T_p was plotted versus frequency as shown in Fig. 7(b) and the curves with different field amplitude were fitted with the function of $T_p = A^*\omega^n$, where ω is the frequency and n is a parameter relating to the slope of T_p. T_p does not show dependence on Fig. 7(b) and the value of n is shown in Table2.

4 Conclusion

The morphological properties of $[Y_{0.8}Ca_{0.2}](Ba_{0.5}Sr_{0.5})_2Cu_3O_{7-\delta}$ were characterized with SEM, TEM, and XRD with Rietveld analysis. AC susceptibilities of $[Y_{0.8}Ca_{0.2}](Ba_{0.5}Sr_{0.5})_2Cu_3O_{7-\delta}$ were characterized and field amplitude/frequency behaviors were investigated. Unlike YBCO, co-doped $[Y_{0.8}Ca_{0.2}](Ba_{0.5}Sr_{0.5})_2Cu_3O_{7-\delta}$ does show only field amplitude dependence, implying that the bulk pinning losses in the sample due to the vortices motion in/out grain boundary is the

dominant factor in ac loss. A- and B-site doping in YBCO changes ac loss mechanism.

Acknowledgements The work in Peru has been supported by the Superior Council of Research of the National University of San Marcos (Grant No. 151301031). This work was also supported by the National Research Foundation of President Post-doctoral fellowship Program (NRF-2013R1A6A3A060443).

References

1. M. K. Wu, J. R. Ashburn, C. J. Torng, P. H. Hor, R. L. Meng, L. Gao, Z. J. Huang, Y. Q. Wang, and C. W. Chu, Phys. Rev. Lett. 58, 908 (1987).
2. V. P. S. Awana, A. Tulapurkar, S. K. Mallik, and A. V. Narlikar, Phys. Rev. B 50, 594 (1994).
3. B. Fisher, J. Genossar, C. G. Kuper, L. Patlagan, G. M. Reisner, and A. Knizhnik, Phys. Rev. B 47, 6054 (1993).
4. T. Wada, T. Sakurai, N. Suzuki, S. Koriyama, H. Yamauchi, and S. Tanaka, Phys. Rev. B 41, 11209 (1990).
5. G. M. Zhao, A. P. B. Sinha, and D. E. Morris, Physica C 297, 23 (1998).
6. R. V. Sarmago and B. G. Singidas, Supercond. Sci. Technol. 17, 5578 (2004).
7. H. Salamati and P. Kameli, J. Magn. Magn. Mater. 278, 237 (2004).
8. R. Giri, V. P. S. Awana, H. K. Singh, R.S. Tiwari, O. N. Srivastava, A. Gupta, B. V. Kumaraswamy, and H. Kishan, Physica C 419, 101 (2005).
9. A. M. Saleh, Pure Sci. Eng. 7, 37 (1998).
10. X. F. Li, J. C. Grivel, A. B. Abrahamsen, and N. H. Andersen, Physica C 477, 6 (2012).
11. M. Tinkham, Introduction to superconductivity, 2nd edition (McGraw-Hill, New York, 1996).
12. K. H. Müller, B. W. Ricketts, J. C. Macfarlane, and R. Driver, Physica C 1177, 162 (1989).
13. J. H. P. M. Emmem, G. M. Stollman, and W. J. M. Dejong, Physica C 169, 418(1990).
14. L. S. Lakshmi, M. P. Staines, K. P. Thakur, R. A. Badcock, and N. J. Long, Supercond. Sci. Technol. 23(6), 065008 (2010).
15. M. Polak, J. Kvitkovic, P. Mozola, E. Usak, P. N. Barnes, and G. A. Levin, Supercond. Sci. Technol. 20(9), S293 (2007).
16. K.-H. Müller, Physica C: Superconductivity, 168, 585 (1990).
17. E. K. Nazarova, A. J. Zaleski, K. A. Nenkov, and A. L. Zahariev, Physica C 468(13), 955 (2008).
18. V. H. Barinotto C., B. L. Willems, A. Bustamante D., L. De los Santos V., and J. Gonzalez G., Physica C 408, 58 (2004).
19. A. Bustamante Domínguez, L. De Los Santos Valladares, B. L. Willems, V. H. Barinotto Call-Cardenas, J. C. González, and X. Obradors, J. Phys. Chem. Solids 67, 594 (2006).
20. A. Bustamante Domínguez, A. M. Osorio Anaya, L. de los Santos Valladares, H. Carhuancho, J. C. González, G. R. C. Cernicchiario, and J. A. Feijoo Levano, Adv. Sci. Technol. 47, 37 (2006).
21. R. A. Young, The Rietveld Method. International union of crystallography book series, Oxford University Press, 1995, ISBN 0198559127, 9780198559122.
22. J. Rodriguez-Carbajal, Crystallographic tools for Rietveld, profile matching and integrated intensity refinements of X-ray and/or neutron data (http://www.ill.eu/sites/fullprof/).
23. C. K. Poole, Handbook of Superconductivity (Academic Press, 2000).
24. L. De Los Santos Valladares, A. Bustamante Domínguez, J. C. González, J. Feijoo Levano, A. M. Osorio Anaya, T. Mitrelias, Y. Majima, and C. H. W. Barnes, Open Supercond. J. 2, 19 (2010).
25. W. H. Li, Phys. Rev. B 56, 5631(1997).
26. Th. Herzog, H. A. Radovan, P. Ziemann, and E. H. Brandt, Phys. Rev. B 56, 2871(1997).
27. R. P. Flippen, T. R. Askew, and M. S. Osofsky, Physica C 201, 391(1992).

Table 1 Atomic positions and occupancies of the sample [Y0.8Ca0.2](Ba0.5Sr0.5)2Cu3O7- obtained by Rietveld refinement. Crystal structure: Orthorhombic (Pmmm). Cell paremeters: a=3.8369Å, b=3.8504Åand c= 11.5388Å(V=170.47$Å^3$) Rietveld factors: R_p= 73.2, R_{wp} = 43.3, R_{exp}= 33.29 and χ^2= 1.69

Atom	Wyckoff	X	Y	Z	Occupancy
Y	1h	0.5	0.5	0.5	0.8
Ca	1h	0.5	0.5	0.5	0.2
Ba	2t	0.5	0.5	0.1877	0.5
Sr	2t	0.5	0.5	0.1877	0.5
Cu1	1a	0	0	0	1
Cu2	2q	0	0	0.3507	1
O1	1e	0	0.5	0	1
O2	2s	0	0.5	0.3547	1
O3	2r	0.5	0	0.3597	1
O4	2q	0	0	0.1659	1

Table 2 Field amplitude versus slope parameter (n) in Figure 7(b)

Field	amplitude	0.5Oe	1Oe	1.5Oe	3Oe
n	0.003	0.0084	0.0099	0.015	

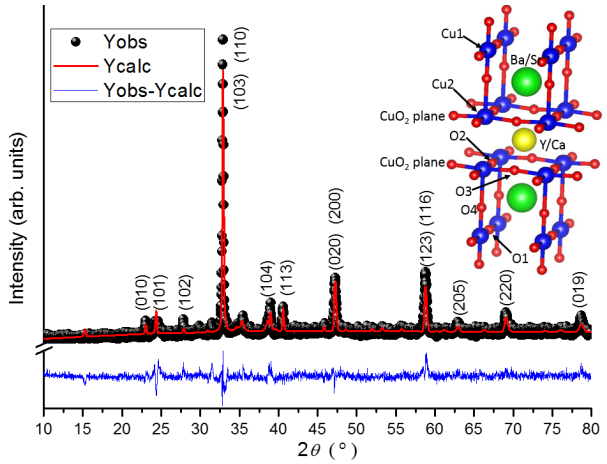

Fig. 1 The XRD spectrum (Yobs) of $[Y_{0.8}Ca_{0.2}](Ba_{0.5}Sr_{0.5})_2Cu_3O_{7-\delta}$ and the Rietveld analysis (Ycalc). The inset is the structure of $[Y_{0.8}Ca_{0.2}](Ba_{0.5}Sr_{0.5})_2Cu_3O_{7-\delta}$.

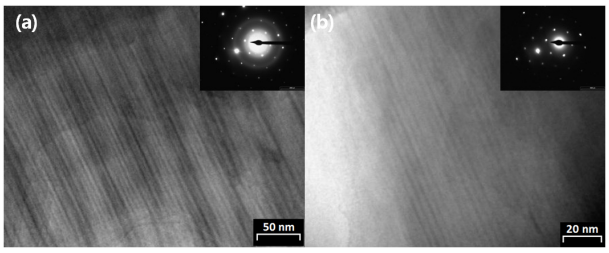

Fig. 2 TEM images of the superconducting $[Y_{0.8}Ca_{0.2}](Ba_{0.5}Sr_{0.5})_2Cu_3O_{7-\delta}$.

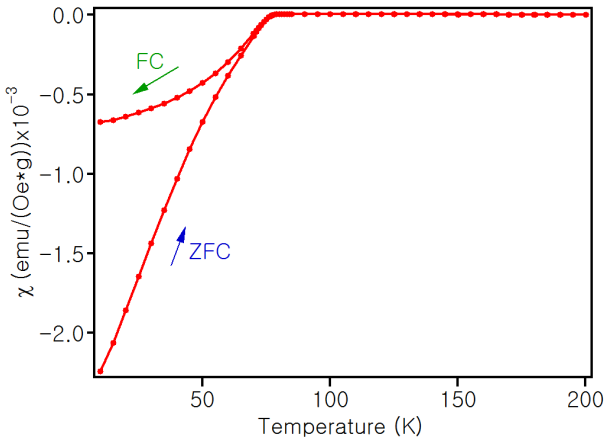

Fig. 3 DC magnetic susceptibility curves of $[Y_{0.8}Ca_{0.2}](Ba_{0.5}Sr_{0.5})_2Cu_3O_{7-\delta}$

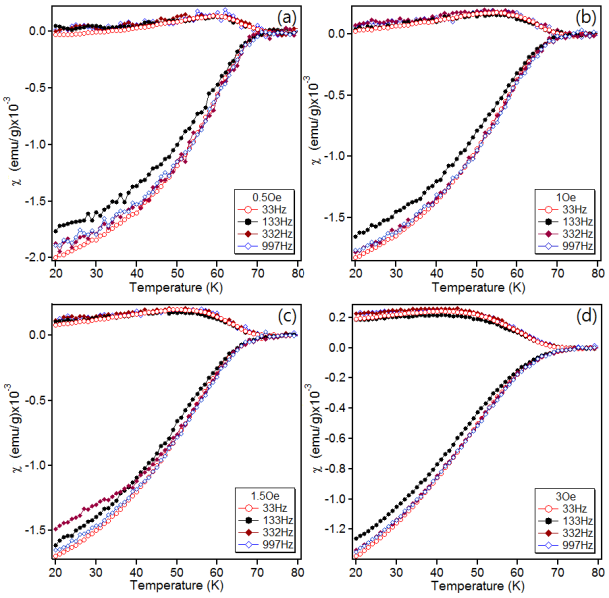

Fig. 4 AC susceptibility curves of $[Y_{0.8}Ca_{0.2}](Ba_{0.5}Sr_{0.5})_2Cu_3O_{7-\delta}$ at different magnetic field amplitudes with varying AC frequencies.

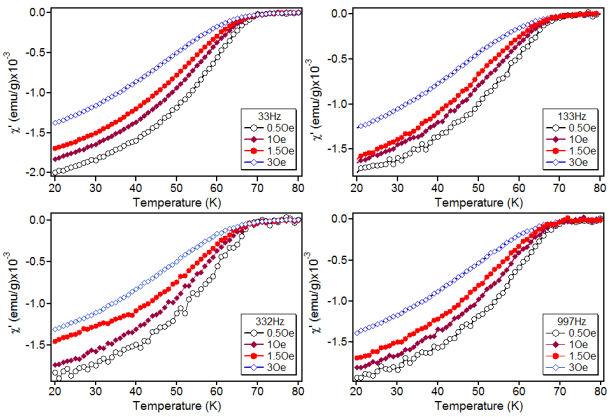

Fig. 5 AC susceptibility curves ($\chi^{'}$) of $[Y_{0.8}Ca_{0.2}](Ba_{0.5}Sr_{0.5})_2Cu_3O_{7-\delta}$ at different AC frequencies with varying AC magnetic field amplitudes.

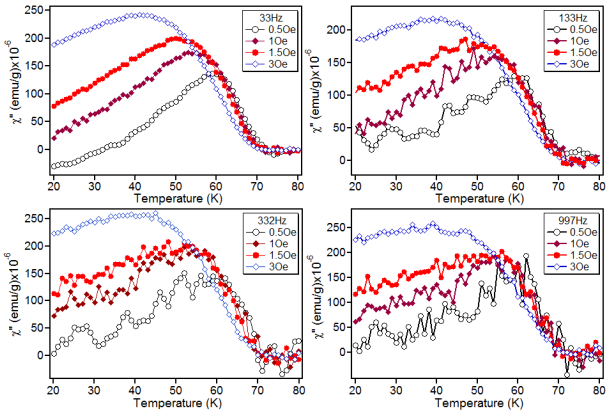

Fig. 6 AC susceptibility ($\chi^{"}$) curves of $[Y_{0.8}Ca_{0.2}](Ba_{0.5}Sr_{0.5})_2Cu_3O_{7-\delta}$ at different AC frequencies with varying AC magnetic field amplitudes.

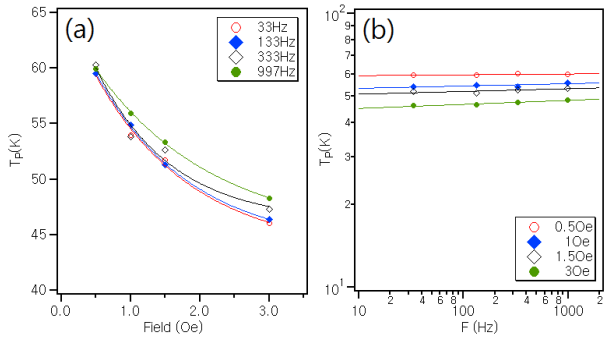

Fig. 7 (a) The field amplitude dependence of T_P in $[Y_{0.8}Ca_{0.2}](Ba_{0.5}Sr_{0.5})_2Cu_3O_{7-\delta}$ with varying frequencies (b) The variation of T_P in $[Y_{0.8}Ca_{0.2}](Ba_{0.5}Sr_{0.5})_2Cu_3O_{7-\delta}$ with varying field amplitude.